ORIGINAL PAPER

Naphthalene group containing side chain liquid crystalline polymers and their rheological behavior

Noordini M. Salleh · Md. Rezaul Karim Sheikh ·
Rosiyah Yahya · Md. Rabiul Karim · Aziz Hassan

Abstract A new polymerizable macromer containing naphthalene ring in the mesogen, 4-butoxyphenyl 6-(6-(methacryloyloxy)hexyl)-2-naphthoate, has been synthesized. The chemical structure of the macromer was confirmed by FTIR, ^{1}H NMR, ^{13}C NMR and liquid crystal behavior was confirmed by polarized optical microscope (POM) and small angle X-ray (SAXS). Results from the POM showed nematic phase appearing at 101.9 °C and smectic phase at 83.8 °C while differential scanning calorimetry (DSC) suggested presence of a wide mesophase range between 50 and 104 °C. This macromer was used to synthesize a series of side-chain liquid crystal polymers (SCLCPs) with different molecular weights having narrow polydispersity (PDI) values via living atom transfer radical polymerization (ATRP). The mesomorphic properties of the liquid crystal macromer and polymers were characterized by POM, DSC and SAXS. In addition, the frequency behavior of the polymers in a smectic phase is characterized by the storage modulus, *G'*, leveling off, at low frequencies. Complex viscosities, |η*| of the smectic phase exhibited a shear thinning behavior over the shear rates investigated.

Keywords Side-chain liquid crystal polymer · Naphthalene · Mesophase · Rheology and smectic

N. M. Salleh · M. R. K. Sheikh (✉) · R. Yahya · M. R. Karim ·
A. Hassan
Department of Chemistry, Faculty of Science, University of
Malaya, 50603, Kuala Lumpur, Malaysia
e-mail: rksheikh@um.edu.my

M. R. K. Sheikh
e-mail: rksheikh@yahoo.com

Introduction

In recent years side chain liquid crystalline polymers (SCLCPs) have been of great interest because of their advantages arising from the properties of the polymer as well as liquid crystal behaviour. Polymers containing mesogenic side groups attached laterally in the main chain are known as side chain liquid crystalline polymers (SCLCPs) because of their liquid crystalline bulk properties [1]. SCLCPs exhibit unique properties such as high heat resistance, flame retardant, chemical resistance, dimensional stability, moldability, heat aging resistance, adhesion, low viscosity, weldable and comparatively low cost. The properties of SCLCPs depend on the different parameters, such as, the nature and length of the spacer, the type of mesogen [2–4], and the nature of polymer backbone. In 1978, Ringsdorf et al. [5–7] developed the first side chain liquid crystal polymer and since then research in polymer liquid crystalline science and technological applications have dramatically increased. The macromolecular structure of SCLCPs depends on both the composition of the polymer main chain and the side chain with liquid crystalline character. Thus, the design and synthesis of SCLCPs can be fulfilled via proper selection of different polymer main chains and side chains to meet the practical applications.

Atom transfer radical polymerization (ATRP) is one of the most efficient, nitroxide-mediated and stable controlled/living-radical polymerization methods that have been used recently [8–11]. This method has been chosen in this study because it can be easily applied to a wide number of monomers which lead to polymer architectures with narrow polydispersities resembling living nature [12–14].

Recently, Jeyasheela and Subramaniam [15] synthesized SCLCPs containing chalcone moiety as a side group by free-radical polymerization using BPO as an initiator. They

found good liquid crystalline and photolithographic properties of the synthesized polymers. On the other hand, Yang and Chang [16] studied the linear viscoelasticity and steady shear behavior of smectic phase of SCLCPs with a polysiloxane backbone. The smectic phase of the SCLCPs exhibited some interesting features such as an orientation under shear and a plateau in the terminal zone of dynamic shear modulus.

In our work, we have synthesized a new macromer having naphthalene moiety and optically active species in the mesogen. SCLCPs of the macromer were synthesized by living ATRP. The macromer and SCLCPs were characterized by ^{1}H NMR, ^{13}C NMR and FT-IR to confirm the chemical structures. The liquid crystal behavior of the macromer and polymers were investigated by POM, DSC, and SAXS. Molecular weight was measured by gel permeation chromatograph (GPC). Rheological studies were done as the measurements of viscoelastic properties can provide information on the local dynamics of the mesogens and the synthesized polymer chain.

Experimental

Materials

Chemicals and solvents were of reagent grades and purchased from Aldrich, Merck, ACROS, R&M Chemicals and J. T. Baker. Acetone and methanol were distilled and kept anhydrous before used. Catalyst copper (I) bromide was purified successively by stirring in acetic acid and ethanol, and then dried. All of the other chemicals and solvents were used as received.

Measurements

^{1}H NMR and ^{13}C NMR measurements were performed with a JEOL spectrometer (Lambda 400 MHz). The FT-IR spectra of the macromer were recorded with a Spotlight 400 Perkin Elmer spectrometer with 16 scanning numbers using attenuated total reflectance (ATR) method. The wavelength was recorded from region 650 to 4000 cm^{-1} at room temperature. Thermal data were obtained using a Perkin Elmer Hyper DSC instrument. Each sample was heated and cooled at a scanning rate of 10 °C/min under nitrogen atmosphere. The second heating and cooling runs were evaluated. The thermal decomposition temperature data were recorded under nitrogen atmosphere at a heating rate of 10 °C/min with a SDT Q600 thermogravimetric analyzer (TA Instrument). The liquid crystal phase transitions were investigated by an Olympus BH-2 polarized light microscope (POM) equipped with Mettler Toledo hot stage FP-82 and the temperature scanning rate was determined at a rate of 1 °C/min. Small-angle X-ray

scattering (SAXS) experiments were performed with Nano-Viewer equipped with a CCD camera (Rigaku Corp. Japan). The X-ray experiment was performed by using the Cu K$_\alpha$ radiation beam (λ=1.541 Å) which was converged and monochromatized by a Confocal Max Flax (CMF) mirror. X-ray generator was a Rigaku Micro7 rotating anode generator (40 kV, 30 mA). The diameter of the X-ray beam controlled by a 3-slit optical system was set to 250 μm. The pellet sample was wrapped with aluminium foil and placed to the instrument. The temperature of a pellet sample was controlled with a hot stage (Mettler Toledo Inc. Switzerland) with accuracy of ±0.1 °C. Molecular weight determinations were performed using a gel permeation chromatography (GPC) instrument (Waters 2414 refractive index detector coupled with a Waters 717 plus Auto-sampler and Waters 600 Controller) with polystyrene standards as reference and tetrahydrofuran (THF) as the eluent. The rheological behavior of the polymers was investigated using a Rheometer Physica MCR301 with 15 mm parallel plates. Prior to any test the zero-gap between the parallel plates was calibrated at 5 °C above their clearing temperature. In the measurements, the sample was placed between preheated fixtures and 15 min were allowed to reach thermal equilibrium, before the gap was set to 0.2 mm. For temperature changes, the control system needed about 5 min to reach a target equilibrium temperature with an error of 1~2 °C. For dynamic oscillatory shearing the linear viscoelastic region of 0.1 % strain was first obtained by strain sweep tests and no pre-shear was applied.

Synthesis of macromer

Synthetic routes for the target macromer are shown in Scheme 1.

Reaction conditions:

a) i. p-Butoxyphenol, ii. Toluene/conc. H$_2$SO$_4$, HBO$_3$ iii. Reflux for 48 h with Dean-Stark trap
b) i. K$_2$CO$_3$/acetone, ii. Br-CH$_2$-CH$_2$-CH$_2$-CH$_2$-CH$_2$-CH$_2$-Br
c) i. KHCO$_3$
d) i. Hydroquinone/DMF ii. 100 °C for 24 h.

Synthesis of 4-butoxyphenyl 6-hydroxynaphthalene-2-carboxylate (1)

In a 250 ml two necks round bottom flask, p-butoxyphenol (0.032 mol) and 6-hydroxy-2-napthaonic acid (0.038 mol) were added in 50 ml dried toluene. Concentrated sulfuric (0.003 mol) and boric (0.003 mol) acids were added subsequently. The mixture was then refluxed for 48 h using Dean-Stark trap to remove the produced water. After completion of the reaction, the solvent was removed under reduced

Scheme 1 Synthetic route of the macromer (DM1)
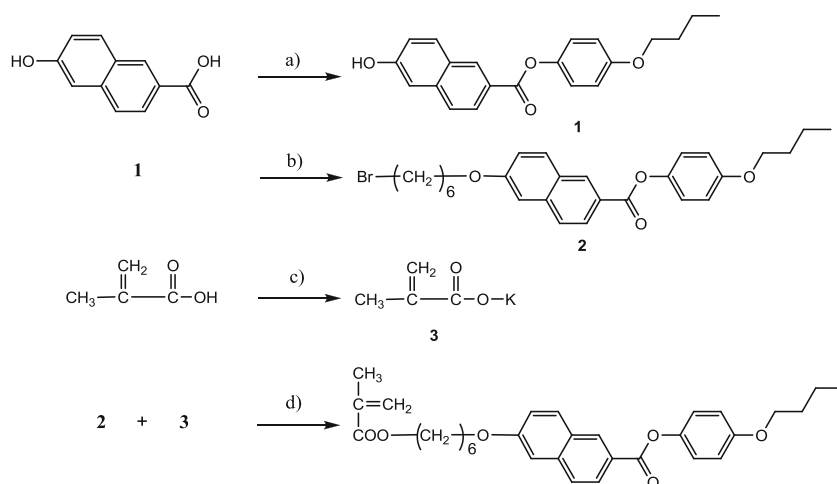
pressure and the product was washed with a mixture of petroleum ether (40–60 °C) and n-hexane (1:1). Acetonitrile was then added into the reaction mixture and heated to dissolve the product. The insoluble solid was then removed by hot filtration. The filtrate was then kept at 0 °C for 12 h and the solid was re-filtered. The solid was again dissolved in hot toluene and filtered to remove unreacted 6-hydroxy-2-naphthaonic acid. The filtrate was then kept at 0 °C for 12 h and the product was filtered to get white crystal product. The product was dried at 40 °C under vacuum with 40 % yield. Mp: 180 °C. ^{1}H NMR, δ (ppm, DMSO, 400 MHz) 10.3 (H, s, Np-OH), 8.7 (H, s, Np-H), 7.8–8.1 (3H, m, Np-H), 7.2 (4H, m, Ph-H), 7.0 (2H, m, Ph-H), 3.9 (t, 2H,−OCH$_2$−), 1.65-1.72 (m, 2H, −CH$_2$−), 1.39–1.48 (m, 2H, −CH$_2$−), 0.89-0.94 (m, 3H, −CH$_3$). ^{13}C NMR, δ (ppm, DMSO, 100 MHz) 131.1 (−OC=O−), 126.3, 125.1, 122.4, 119.5, 114.6, 108.5 (aromatic carbons), 67.2, 30.5, 18.5 (−CH$_2$−), 13.4 (−CH$_3$).FT-IR, 3480 (−OH), 2873–2960 (alkyl), 1710 (−C=O), 1434–1500 (−C=C− Ar), 1185 (ester), 800–875 (p-Ar) cm^{-1}.

Synthesis of 4-butoxyphenyl 6-(6-bromohexyloxy)-2-naphthoate (2)

In a 250 ml two necks round bottom flask, a mixture of (1) (0.02 mol), 1,6-dibromohexane (0.20 mol), potassium carbonate (0.02 mol) and distilled acetone (50 ml) was refluxed under stirring for 24 h. After completion of the reaction, the reaction mixture was filtered and the precipitate washed thoroughly with acetone. The acetone was then removed under reduced pressure. After removing solvent, a mixture of petroleum ether (40–60 °C) and hexane (1:1) was added. The precipitate was filtered off and recrystallized twice from ethanol with hot filtration. The white solid product was dried at 40 °C under vacuum to give 67 % yield. Mp: 80 °C. ^{1}H NMR, δ (ppm, CDCl$_3$, 400 MHz) 8.69 (s, 1H, Np-H), 8.13–8.16 (dd, 1H, Np-H), 7.78–7.93 (dd, 2H, Np-H), 7.14–7.24

(m, 4H, Ar-H), 6.93–7.00 (m, 2H, Ph-H), 4.11–4.14 (t, 2H, −OCH$_2$−), 3.97–4.00 (t, 2H, −CH$_2$-Br), 3.43–3.47 (t, 2H, Ar-CH$_2$−), 1.86–1.97 (m, 4H, −CH$_2$−), 1.76–1.83 (m, 2H, −CH$_2$−) 1.4–1.5 (m, 6H, −CH$_2$−), 0.89–0.94 (m, 3H, −CH$_3$). ^{13}C NMR, δ (ppm, CDCl$_3$, 100 MHz) 131.6 (−OC=O−), 131.0, 127.0, 126.2, 122.5, 120.0, 115.1, 106.5 (aromatic carbons), 68.1 (−CH$_2$−), 33.8, 32.7, 31.4, 29.0, 27.9, 25.4, 19.3 (−CH$_2$−13.9 (−CH$_3$). FT-IR, 2865–2932 (alkyl), 1730 (−C=O), 1390–1500 (−C=C− Ar), 1197 (ester), 811–859 (p-Ar) cm^{-1}.

Synthesis of 4-butoxyphenyl 6-(6-(methacryloyloxy) hexyl)-2-naphthoate (DM1)

In a 250 ml two necks round bottom flask, methacrylic acid (3.35 mmol) was added slowly to potassium hydrogen carbonate (3.35 mmol) at room temperature to form potassium methacrylate. A solution of (2) (2.24 mmol) and hydroquinone (0.025 mmol) in DMF (50 ml) was added slowly into the previously prepared potassium methacrylate solution. The reaction mixture was heated with stirring at 100 °C for 24 h. Thereafter the solvent was removed under vacuum followed by addition of 100 ml water at room temperature. The solid was again filtered and dissolved in dichloromethane. The organic phase was washed twice by 5 % NaOH solution and twice by distilled water, followed by solvent removal under reduced pressure. The white solid was filtered and recrystallized twice from ethanol and dried at 40 °C under vacuum to give 55 % yield. Mp: 103 °C. ^{1}H NMR, δ (ppm, CDCl$_3$, 400 MHz) 8.61 (s, H, Np-H), 8.05–8.08 (dd, 1H, Np-H), 7.70–7.81 (dd, 2H, Np-H), 7.05–7.15 (m, 4H, Ar-H), 6.85–6.89 (m, 2H, Ph-H), 6.03 (H, s, =CH$_2$), 5.46–5.48 (m, H, =CH$_2$) 4.09–4.12 (t, 2H, -OCH$_2$−), 4.02–4.06 (t, 2H, Ph-CH$_2$−), 3.88–3.92 (t, 2H, Ar-CH$_2$−), 1.86–1.87 (t, 3H, -CH$_3$) 1.78–1.85 (m, 2H, -CH$_2$−), 1.63–1.74 (m, 4H, -CH$_2$−) 1.4–1.5 (m, 6H, -CH$_2$−), 0.89–0.94 (t, 3H, -CH$_3$). ^{13}C NMR, δ (ppm, CDCl$_3$, MHz) 131.6, 130.9 (−OC=O), 126.9, 126.1, 122.4,

Table 1 Polymerization of Macromer DM1

Sample	$[M]_0/[I]_0/$ $[C]_0/[L]_0$[a]	M_w (Cal.)	M_w (GPC)[b]	PDI (M_w/M_n)[b]
DP1M1	40/1/1.5/2	20,184	10,475	1.17
DP2M1	60/1/1.5/2	30,276	10,163	1.16
DP3M1	80/1/1.5/2	40,368	12,817	1.16

[a] Feed molar ratio; [M] macromer; [I] initiator; [C] catalyst; [L] ligand

[b] Molecular weights and polydispersity index (PDI) values were measured by GPC, using THF as an eluent, polystyrene as a standard. M_n, number average molecular weight; M_w, weight average molecular weight

120.0, 115.1, 106.5 (aromatic carbons), 125.0 (C), 68.1, 64.6 ($-CH_2-$), 31.3, 29.0, 28.5, 25.7, 19.2 ($-CH_2-$), 18.3, 13.9 ($-CH_3$). FT-IR, 2871–2932 (alkyl), 1709–1730 ($-C=O$), 1390–1500 (C=C Ar), 1197 (ester), 811–859 (p-Ar) cm^{-1}.

Synthesis of polymers

Polymers (DP1M1–DP3M1) were synthesized by living ATRP by using 2-bromoisobutyrate (EBriB), CuBr and N, N,N',N',N"-pentamethyldiethylenetriamine (PMDETA) as an initiator, catalyst and ligand respectively.

Polymer DP1M1

CuBr (0.05 mmol), and macromer DM1 (1.3 mmol) were added to a three neck round bottom flask. The flask was sealed with a rubber septum, degassed and back-filled with nitrogen gas three times. 2 ml deoxygenated anisole was added via syringe, followed by deoxygenated PMDETA (0.064 mmol). After stirring for 30 min at room temperature, the reaction mixture was placed in a preheated oil bath at 90 °C for 7 h. The solution turned light green as the CuBr/PMDETA complex was formed. After the majority of the metal complex had formed, ethyl 2-bromoisobutyrate (EBriB) (0.032 mmol) was added to the reaction flask. The solution was then passed through a neutral Al_2O_3 column with THF as an eluent to remove the catalyst, CuBr. The product was concentrated under reduced pressure and precipitated twice into 15 fold excess of methanol. The white product of polymer was collected by filtration and dried under vacuum. $M_w=10,475$ g/mol and PDI $(M_w/M_n) = 1.17$.

Polymer DP2M1

Polymer DP2M1 was synthesized according to the procedure described for polymer DP1M1 except for the amount of initiator, EBriB (0.0211 mmol). $M_w=10,163$ g/mol and PDI $(M_w/M_n) = 1.16$.

Polymer DP3M1

Polymer DP3M1 was synthesized according to the procedure described for polymer DP1M1 except for the amount of initiator, EBriB (0.0159 mmol). $M_n=12,817$ g/mol and PDI $(M_w/M_n) =1.16$.

Fig. 1 ^{1}H NMR spectra of (a) macromer DM1 and (b) polymers DP1M1-DP3M1 in CDCl$_3$
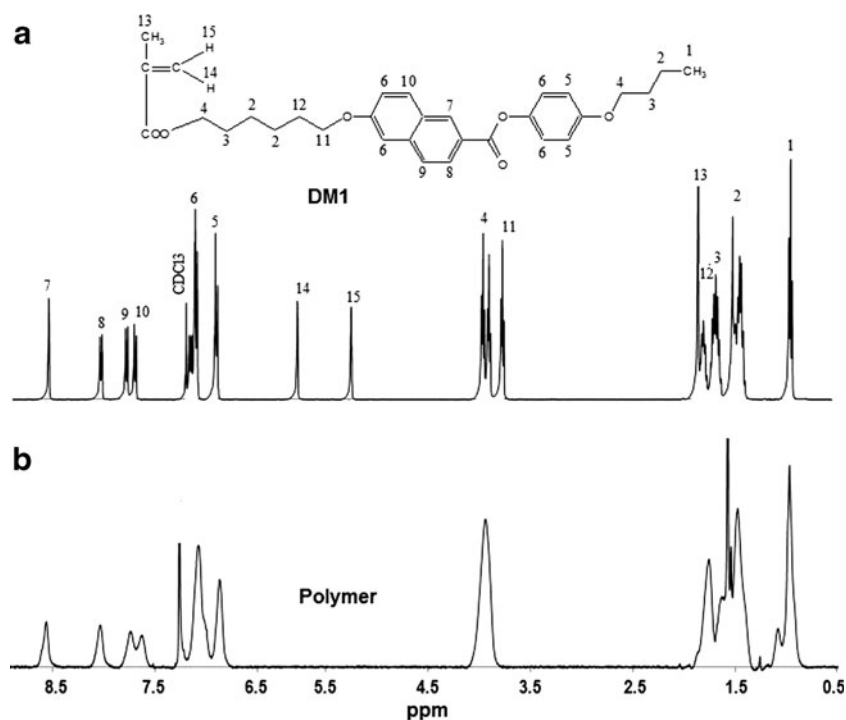
Table 2 Phase behavior and thermal properties of macromer and polymers

Sample	Phase transitions(°C)[a,b] (corresponding enthalpy changes, J g⁻¹)	
	Heating	Cooling
DM1	g 49.9 S 86.8 (0.97) N 103.6 (0.96) I	I 102.3 (−1.04) N 85.5 (−1.02) S
DP1M1	g 62.8 S 149.4 (1.39) N 162.8 (2.48) I	I 161.6 (−2.27) N 148.2 (−1.24) S
DP2M1	g 62.6 S 149.1 (1.41) N 162.6 (2.32) I	I 161.3 (−2.43) N 147.9 (−1.15) S
DP3M1	g 68.4 S150.6 (0.97) N 163.3 (1.82) I	I 162.01 (−2.08) N 149.3 (−1.44) S

[a] Transition temperatures (°C) and enthalpies (in parentheses, J g⁻¹) were measured by DSC (at a heating and cooling rate of 10 °C/min)

[b] g glassy; S Smectic phase; N nematic phase; I isotropic phase

Results and discussion

Synthesis and characterization

A macromer with electron releasing (−OC$_4$H$_9$) terminal group was synthesized by acid-catalyzed esterification [17, 18] of 4-butoxyphenol and 6-hydroxy-2-napthaonic acid. The synthetic route for the macromer DM1 is outlined in Scheme 1. ATRP has been proven to be a successful polymerization technique to prepare polymers for a variety of monomers with narrow polydispersity [10, 19, 20]. All polymers were prepared using CuBr, PMDETA, and EBriB as the catalyst, ligand and initiator respectively in anisole and the reaction conditions were all kept at 90 °C for 7 h. The relative molecular weights and polydispersity index (PDI) values of the polymers were determined by GPC. The polymerization conditions and GPC results are shown in Table 1.

The macromer and polymers had good solubility at room temperature in common organic solvents, such as tetrahydrofuran, ethyl acetate and dichloromethane. Since the macromer had good solubility in methanol, it was chosen to remove unreacted macromer from polymers in the normal precipitation process. The chemical structures of the macromer and polymers were confirmed by ¹H NMR spectroscopy as shown in Fig. 1. The spectral assignments clearly supported the proposed structures: DM1 showed characteristic proton peaks of the vinyl groups at 5.48–6.03 ppm (denoted as *14* and *15* in

(Fig. 1a), the sharp and clearly separated proton resonances of macromer disappeared after polymerization (Fig. 1b), while broad and overlapped resonances of LC mesogen attached to polymeric back bones appeared at nearly the same positions.

Liquid crystalline properties

The thermal properties and the phases of the macromer and polymers were studied by DSC, POM and SAXS. The phase transition temperatures and changes in enthalpy (ΔH) obtained during the first cooling and the second heating cycles are summarized in Table 2. The enthalpy changes observed are nearly independent of the molecular weights and this observation is in agreement with results obtained by Trimmel et al. [21]. They found that the polymers containing more than ten repeating units gave independent enthalpy changes to the molecular weight but were strongly dependent on spacer length, with a minimum $n=6$. From the data listed in Table 2, the mesophase temperature ranges of polymers are greater than the macromer. This indicates that the polymerization effect can stabilize and widen the mesophase temperature range and that the increase in molecular weight definitely increases the mesomorphic-mesomorphic and mesomorphic-isotropic phase transition temperatures.

Figure 2 represents the DSC thermograms of heating and cooling cycles of the macromer at a rate of 10 °C/min. The macromer exhibits a glass transition temperature, T_g, at

Fig. 2 DSC thermograms for the macromer DM1
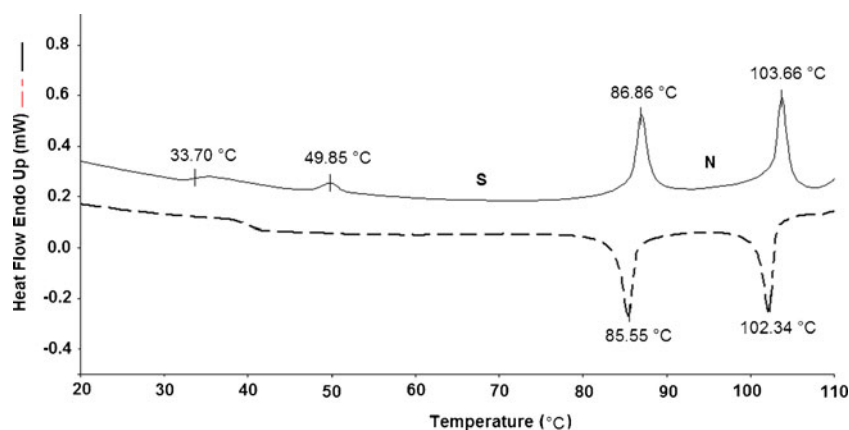
33.7 °C followed by a nematic and smectic mesophases which undergo isotropization at 103.6 °C during second heating scan. The thermal transitions are enantiotropic, where the liquid crystal phase exists upon heating and cooling. Two peaks at 102.3 °C and 85.5 °C associated with the isotropic-nematic and nematic-smectic transitions respectively are observed during the cooling scan. Figure 3 shows the POM of macromer texture obtained at different temperatures. Upon cooling from isotropic melt, schlieren texture of nematic mesophase appears at 101.9 °C (Fig. 3a). Certain region of focal conic fan texture which is characteristic of a smectic mesophase at 83.8 °C becomes dark indicating the isotropic liquid area (Fig. 3b). When the macromer is cooled to room temperature from its isotropic state, it solidifies and its crystalline phase appears lumber-like mosaic textures (Fig. 3c). The mesophase temperature range is found to be very broad (49.85–103.66 °C) which might be attributed to the presence of crankshaft structure of the naphthalene that can decrease the freedom of molecule movement [22].

Figure 4 represents the DSC thermograms of heating and cooling cycles of polymers at rate of 10 °C/min. All the polymers enter the nematic mesophase at 148 °C and smectic mesophase at 161 °C during the cooling scans. Figure 5 represents the POM textures of the polymers upon cooling from isotropic point. The schlieren textures appear with droplets when the polymers were cooled at 165.7 °C from isotropic temperature as shown in Fig. 5a. The droplets are characteristic of nematic mesophase because they occur nowhere else [23]. There are many point singularities with two dark brushes in the schlieren textures, which further confirm the nematic nature of the mesophase because such singularity is not compatible with the smectic C phase [24, 25]. Upon further cooling, coarse textures of disclination loops are formed (Fig. 5b). The stripes of the textures disappear upon heating and regenerated by cooling. When the polymers are cooled at 108 °C, the striped loops grow to striated feather textures (Fig. 5c).

SAXS experiments were performed to elucidate the mesophase textures. Figure 6 shows the SAXS intensity
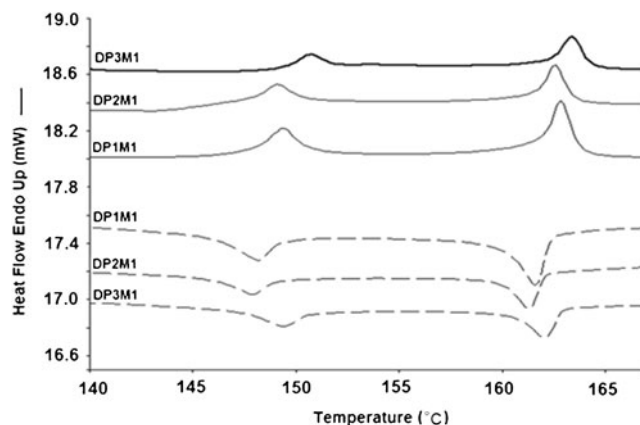
Fig. 4 DSC thermograms for the polymers

profiles of macromer DM1 at room temperature and 100 °C. At room temperature, the sample shows a sharp scattering signal in the low q region (2.2 nm^{-1}) indicating a typical smectic phase texture and an intense broad peak in the higher q region (3.27 nm^{-1}) which indicates that only a short-range order exists in the molecular lateral packing [26]. The layer periodicities calculated for the first sharp peak are 2.86 nm and 1.92 nm for the broad peak. After heating at 100 °C, the sharp peak disappears while the broad peak remains, indicating that the sample has entered the nematic phase. From the results of DSC, POM and SAXS, we can conclude that the transitions from isotropic to nematic phase has occurred at higher temperature and that from nematic to smectic phase has occurred at lower temperature.

Rheological properties

Determination of linear viscoelastic (LVE) region of materials is important in performing dynamic rheological characterizations which are independent of applied strains. Figure 7 shows the strain dependence of storage (G') and loss (G'') moduli of the polymers at 170 °C with $\omega=10$ rad/s
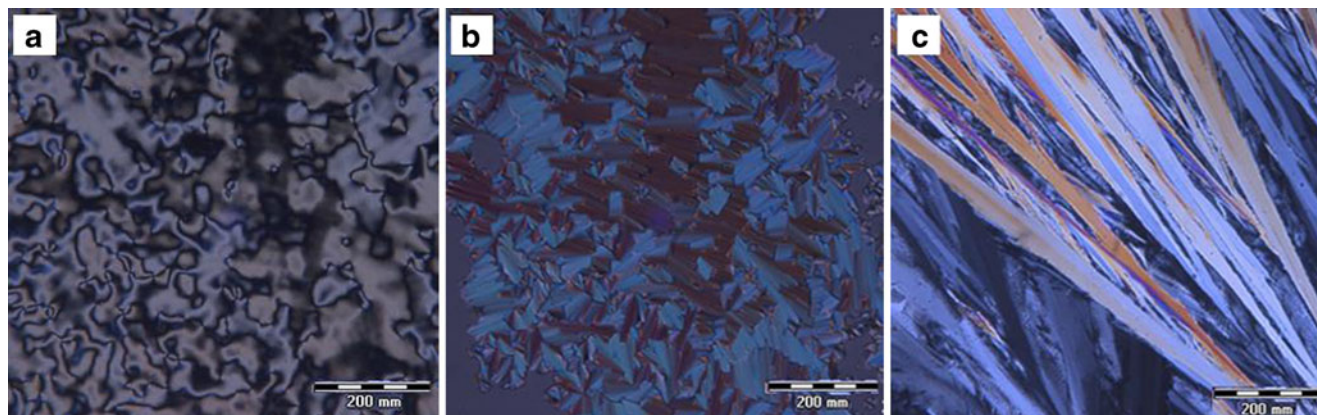
Fig. 3 POM textures of macromer DM1. **a** Nematic at 101.9 °C (**b**) Smectic at 83.8 °C (**c**) Crystalline at room temperature
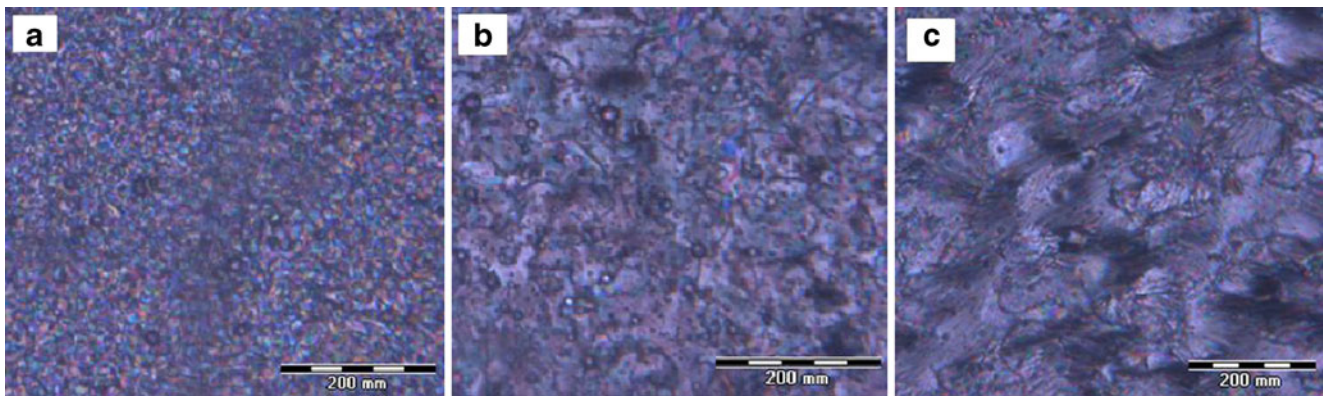
Fig. 5 POM textures of polymer DP1M1. **a** 165.7 °C (**b**) 162 °C (**c**) 108 °C

by strain amplitude sweep experiments. It can be seen that G'' is greater than G' in both polymers and largely insensitive to strain amplitude. As such, the polymers do not form a viscoelastic gel.

Figure 8 represents the viscosity properties of the polymers over the temperature range of phase transitions. Both polymers exhibit Bingham body-like flow behavior at 100 °C and 110 °C which shows "three region flow curves" as characterized by Onogi and Asada [27, 28]. At low values of shear rate ($\dot{\gamma} <1\ s^{-1}$), both polymers exhibit a shear thinning behavior and the viscosity decreases. A Newtonian behavior appears at intermediate values of shear rate ($1\ s^{-1} <\dot{\gamma} <10\ s^{-1}$), where the domains appear to decrease in size with increasing shear rate. At this stage the viscosity is relatively insensitive to shear rate. At higher values of ($\dot{\gamma} >10\ s^{-1}$), a strong thinning behavior appears where the domain structure is not evident at this stage [27]. These results are in agreement with the results of Kannan et al. [29] and Dan et al. [30] which suggested that the large amplitude oscillatory shear orientated the SCLCPs.

However, as the temperature is increased from 120 °C to 150 °C, the polymers exhibit shear thinning behavior where the particles rearranged resulting in reduced flow resistance and consequently lower the viscosity of the polymers with increased in shear rate. The polymers exhibit Newtonian behavior at low shear rate, followed by strain hardening behavior at higher shear rate at 160 °C and 170 °C which are in the isotropic region for both polymers. Rubin et al. [31] reported that the strain hardening behavior is probably due to the tendency of the mesogens to orient perpendicular to the backbone in the SCLCPs. The mesogens which are attached to a strand may be forced to adopt an intermediate orientation between the backbone segment and local orientation of the director.

Figure 9 shows plots of log G' vs log ω and plots of log G'' vs log ω for polymer DP2M1 at 100 °C to 150 °C in the smectic region and 160 °C in the nematic region. The values of G' and G'' in the smectic region are much higher than those in the nematic region, attributing to the 3-dimensional textures in smectic textures and 1-dimensional textures in the nematic phase. This finding is similar to that of Kim and Han [32] who studied the effect of bulkiness of pendant side group semiflexible main-chain liquid crystal polymers (MCLCPs).
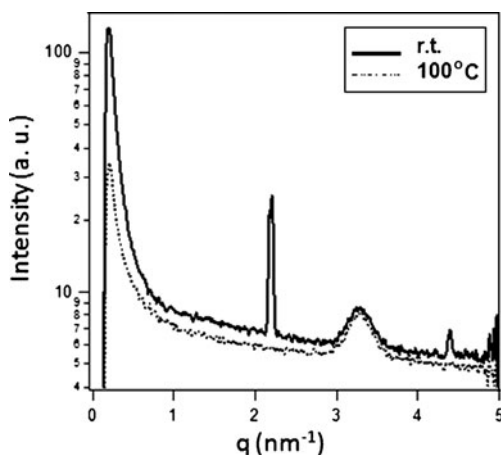

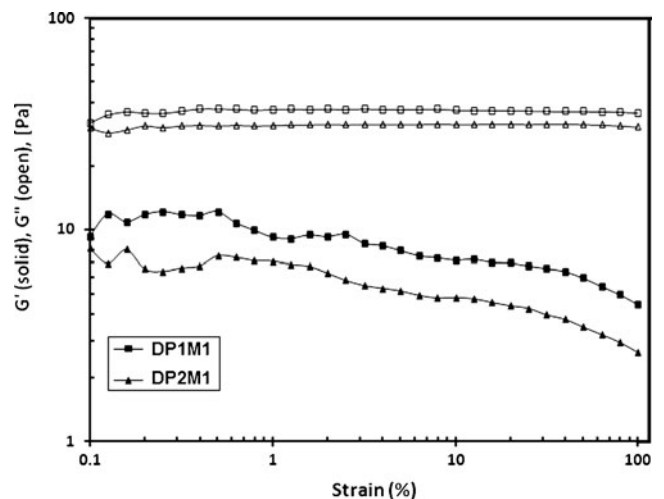**Fig. 6** Small angle X-ray scattering of macromer DM1
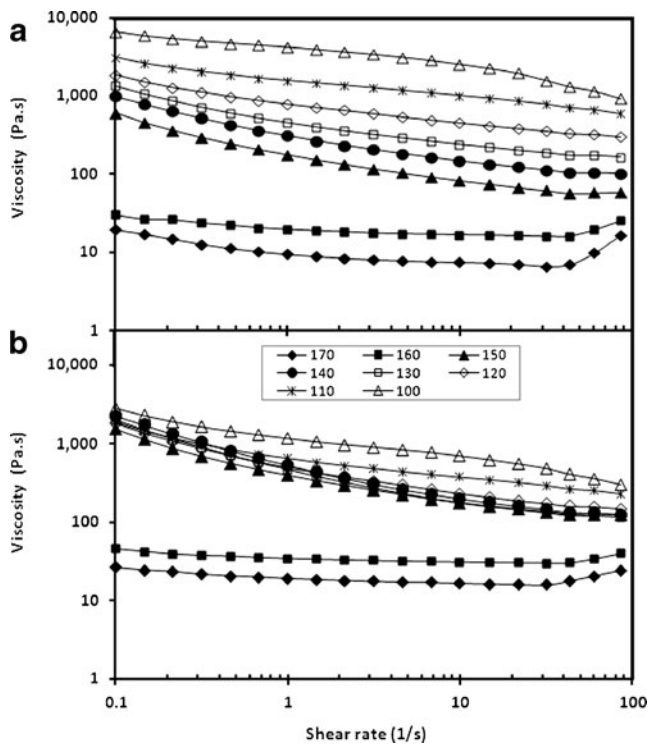

Fig. 7 Strain amplitude sweep of polymers at 170 °C

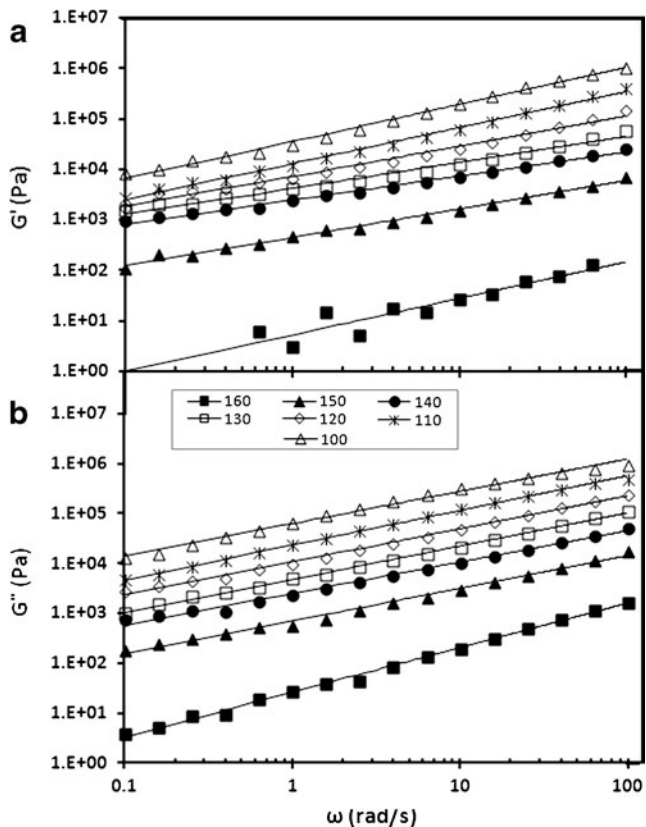**Fig. 8** Viscosity of polymers (**a**) DP2M1 (**b**) DP3M1 at various temperatures

Fig. 9 Plots of log G' vs log ω and log G'' vs log ω for polymer DP2M1 at various temperatures

At low frequency values, both G' and G'' tend to level off and do not follow the typical terminal behavior where $G' \propto \omega^2$ and $G'' \propto \omega^2$. The slope of G' in the terminal region decreases from 0.73 to 0.56 as the temperature increases from 100 °C to 150 °C. As the temperature increases from 100 °C to 150 °C the slope of the loss modulus G'' decreases from 0.69 to 0.62. From this observation, the polymer exhibits solid-like behavior when $T \leq 150$ °C. The slopes of G' and G'' are subsequently increased to 0.97 and 0.94 respectively when the temperature increases to 160 °C. At this temperature, the polymer exhibits liquid-like behavior. The general trends resemble the unshifted linear visco-elastic data as reported by Auad et al. [33] for the smectic SCLCPs. The changes in the linear viscoelastic response are a common signature of ordering transitions.

In the isotropic phase, molecular weight of a polymer has a strong influence on the rheology where an entanglement plateau emerges. Nevertheless, the polymer, DP2M1, has a low molecular weight which is less than the molar mass of entanglement and also the smectic phase rheology is dominated by the layer structure and is comparatively insensitive to the molecular weight. Therefore, it is not expected to have a plateau in the terminal region. Similar trend of behavior are also obtained for DP3M1 polymer.

Figure 10 shows a plot of log $|\eta^*|$ vs log ω for polymer DP2M1 at various temperatures, where $|\eta^*|$ is the complex viscosity defined by $|\eta^*| = [(G'/\omega)^2 + [(G''/\omega)^2]^{1/2}$. As the temperature increases from 100 °C to 150 °C, the polymer enters the smectic phase which exhibits a strong frequency dependence of $|\eta^*|$ at low angular frequencies and then Newtonian behavior is observed at 160 °C. At this temperature, the polymer enters the nematic phase which exhibits a weak frequency dependence over the entire range of angular frequencies tested. The abrupt decrease of $|\eta^*|$ values is due to
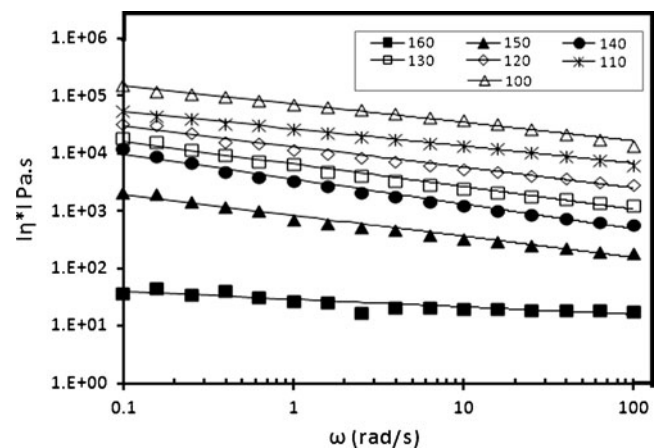

Fig. 10 Plots of log $|\eta^*|$ vs log ω for polymer DP2M1 at various temperatures

breakdown of 3-dimensional smectic order to 1-dimensional nematic order where, in nematic phase the molecules would exhibit preferential orientation during shear flow. A similar observation has been reported by Lee and Han [34] for their SCLCPs.

Conclusions

A new polymerizable macromer having naphthalene moiety and optically active species in the mesogen has been synthesized. A series of side chain liquid crystal polymers (SCLCPs) with different molecular weights and narrow polydispersities derived from this new macromer was successfully prepared by ATRP in anisole. The chemical structures of the macromer and polymers were confirmed by ^{1}H NMR, ^{13}C NMR and FT-IR while evidence of the liquid crystalline behavior of the macromer and polymers were shown by DSC, POM and SAXS. All the synthesized macromer and polymers showed nematic and smectic mesophase with different textures. The viscoelasticity properties carried out in smectic to nematic region showed that the frequency behavior of the polymers in a smectic phase is characterized by the leveling off in the storage modulus, G' at low frequencies. Complex viscosities, $|\eta^*|$ of the smectic phase exhibited a shear thinning behavior over the shear rates investigated.

References

1. Collings P (2002) Princeton Univ. Press, New Jersey

2. Salehli F, Yildiz S, Ozbek H, Uykur E, Gursel YH, Durmaz YY (2010) Polymer 51:1450–1456
3. Anuragudom P, El-daye J, Chinwangso P, Advincula R, Phanichphant S, Lee T (2011) Polym Int 60:660–665
4. Watanabe M, Tsuchiya K, Shinnai T, Kijima M (2012) Macromolecules 45:1825–1832
5. Nair B, Gregoriou V, Hammond P (2000) Polymer 41:2961–2970
6. Wittmann J, Meyer S, Damman P, Dosiere M, Schmidt H (1998) Polymer 39:3545–3550
7. Yuan G, Zhao Y (1997) Polymer 38:119–125
8. Zhang H, Lei X, Su Z, Liu P (2007) J Polym Res 14:253–260
9. Yu W-N, Liu S-X, Wang H-M, Tian R (2012) J Polym Res 19:1–7
10. Wang LY, Li KC, Lin HC (2010) Polymer 51:75–83
11. Xiong L, Liang H, Wang R, Chen L (2011) J Polym Res 18:1017–1021
12. Coessens V, Matyjaszewski K (2010) J Chem Educ 87:916–919
13. Matyjaszewski K (2004) Mol Cryst Liq Cryst 415:23–34
14. Ramakrishnan A, Dhamodharan R (2000) J Macromol Sci, Pure Appl Chem 37:621–631
15. Jeyasheela S, Subramanian K (2012) Mol Cryst Liq Cryst 557:161–175
16. Yang I, Chang S (2002) J Polym Res 9:163–168
17. Lowrance W Jr (1971) Tetrahedron Lett 12:3453
18. Van Meter J, Klanderman B (1973) J Am Chem Soc 95:626–627
19. Patten T, Matyjaszewski K (1998) Adv Mater 10:901–915
20. Wang XZ, Zhang HL, Shi DC, Chen JF, Wang XY, Zhou QF (2005) Eur Polym J 41:933–940
21. Trimmel G, Riegler S, Fuchs G, Slugovc C, Stelzer F (2005) In: Buchmeiser M (ed) Metathesis polymerization. Springer, Berlin
22. Chen BK, Tsay SY (2005) Polymer 46:8624–8633
23. Kong X, Tang BZ (1998) Chem Mater 10:3352–3363
24. Demus D (1999) Wiley-VCH, Germany
25. Stegemeyer H (1994) Springer, Germany
26. Wang Q, Yang C, Xie H, Wang X, Zhang H (2010) Liq Cryst 37:435–443
27. Onogi S, Asada T (1988) In: Astarita G, Marrucci G, Nicolais L (eds) Rheology and rheo-optics of polymer liquid crystals in Rheology. Plenum Press, New York
28. Lee H, Denn M (1999) Korea-Aust Rheol J 11:269–273
29. Kannan R, Kornfield J, Schwenk N, Boeffel C (1993) Macromolecules 26:2050–2056
30. Dan K, Kim B, Han Y (2009) Macromol Res 17:313–318
31. Rubin SF, Kannan RM, Kornfield JA, Boeffel C (1995) Macromolecules 28:3521–3530
32. Kim D, Han C (2000) Macromolecules 33:3349–3358
33. Auad ML, Kempe MD, Kornfield JA, Rendon S, Burghardt WR, Yoon K (2005) Macromolecules 38:6946–6953
34. Lee K, Han C (2003) Macromolecules 36:8796–8810